Simulation of Cold-Test Parameters and RF Output Power for a Coupled-Cavity Traveling-Wave Tube

Jeffrey D. Wilson, *Member, IEEE,* and Carol L. Kory, *Member, IEEE*

Abstract— **Procedures have been developed which enable the accurate computation of the cold-test (absence of an electron beam) parameters and RF output power for the slow-wave circuits of coupled-cavity traveling-wave tubes (TWT's). The cold-test parameters, which consist of RF phase shift per cavity, impedance, and attenuation, are computed with the three-dimensional electromagnetic simulation code MAFIA and compared to experimental data for an existing V-band (59–64 GHz) coupled-cavity TWT. When simulated in cylindrical coordinates, the absolute average differences from experiment are only 0.3% for phase shift and 2.4% for impedance. Using the cold-test parameters calculated with MAFIA as input, the NASA Coupled-Cavity TWT Code is used to simulate the saturated RF output power of the TWT across the V-band frequency range. Taking into account the output window and coupler loss, the agreement with experiment is very good from 60–64 GHz, with the average absolute percentage difference between simulated and measured power only 3.8%. This demonstrates that the saturated RF output power of a coupled-cavity TWT can be accurately simulated using cold-test parameters determined with a three-dimensional electromagnetic simulation code.**

I. Introduction

FOR a number of years, computer simulation has played an important role in the design procedure for coupled-cavity traveling-wave tube (TWT) circuits. The NASA Coupled-Cavity TWT code [1]–[4] in particular has been shown to accurately simulate the RF output power characteristics for several circuit designs [5]–[8]. Despite the use of this and similar models, designing a coupled-cavity traveling-wave tube (TWT) slow-wave circuit was still a long and expensive procedure, because the models required the experimentally obtained input of the individual cavities' electrical characteristics: RF phase shift per cavity, impedance, and attenuation. These characteristics, known as cold-test parameters, needed to be measured for each circuit design iteration.

With the recent advent of three-dimensional electromagnetic simulation codes, it is now possible to simulate each cold-test parameter. In this paper, we show that the saturated RF output power for a coupled-cavity TWT can be accurately simulated with the NASA Coupled-Cavity TWT code using cold-test parameters calculated with the three-dimensional code MAFIA [9]–[11]. The simulated results of each code are compared to experimentally measured results for the Hughes Aircraft Company 961HA TWT, a 59–64 GHz, 75-Watt ferruled coupled-cavity TWT developed under NASA Contract NAS3-25090 [12].

Manuscript received March 28, 1995. The review of this paper was arranged by Associate Editor J. A. Dayton Jr.

J. D. Wilson is with the NASA Lewis Research Center, Cleveland, OH 44135 USA.

C. L. Kory is with the ANALEX Corporation, NASA Lewis Research Center, Cleveland, OH 44135 USA.

IEEE Log Number 9414587.

II. Analysis

A. Cold-Test Parameters

MAFIA (Solution of MAxwell's equations by the Finite-Integration-Algorithm) Version 3.20 is a powerful, three-dimensional, electrodynamic code that is used for the computer-aided design of 2D and fully 3D electromagnetic devices. The Finite Integration Technique (FIT) algorithm produces a set of finite-difference matrix equations for the electric and magnetic field vectors. The solution of these equations yields static, frequency-domain or time-domain solutions of Maxwell's equations. The code includes nine interrelated modules. The cold-test characteristics used as input for the NASA Coupled-Cavity TWT Code were calculated using the M (mesh generator), E (eigenmode solver), and P (postprocessor) modules of MAFIA.

The Hughes 961HA ferruled coupled-cavity slow-wave circuit (Fig. 1) was modeled in both the Cartesian and cylindrical coordinate systems. A MAFIA grid cell resolution of 53 × 53 in the transverse plane and 29 cells per cavity in the axial direction was generated in Cartesian coordinates. A MAFIA mesh of 27 × 37 × 29 in the radial, azimuthal, and axial directions, respectively, was used to model the circuit in the cylindrical coordinate system. The lines of each mesh were made as equally spaced as possible with grid boundaries matching with major geometrical features such as the beam aperture and ferrules. The cylindrical MAFIA mesh is shown for the end and top views in Fig. 2(a) and (b), respectively. The dimensions of the standard cavity of the 961HA ferruled coupled-cavity circuit are listed in Table I of [11].

The method for calculating the RF phase shift per cavity is similar to that of Kantrowitz and Tammaru [13] and Maruschek *et al.* [14] where the frequency-phase dispersion is determined by obtaining resonant frequencies in truncated sections of circuit. One-, two-, and three-cavity sections are truncated perpendicularly to the axial axis. The truncating plane can be either an "electric wall" where the electric field is perpendicular to the boundary or a "magnetic wall" where the magnetic field is perpendicular. Fig. 3 shows a MAFIA three-dimensional view of a two-cavity section of the Hughes 961HA coupled-cavity TWT circuit. The electric field at a phase shift of $5\pi/4$ radians (225°) per cavity is shown with the arrow size proportional to the magnitude of the field.

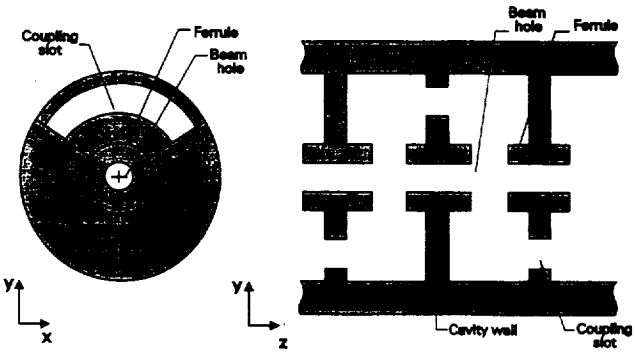

(a) (b)

Fig. 1. (a) End, and (b) cross-sectional view section of a ferruled coupled-cavity TWT slow-wave circuit.

The impedance is a measure of the strength of interaction between an RF wave harmonic and the electron beam. For the nth space harmonic, the on-axis beam interaction impedance [15] is defined as

$$K_n = \frac{E_n^2}{2\beta_n^2 P_{RF}} \tag{1}$$

where E_n is the magnitude of the nth space harmonic of the on-axis electric field, β_n is the axial phase constant for the same harmonic, and P_{RF} is the RF power flow defined by

$$P_{RF} = W v_g \tag{2}$$

where v_g is the group velocity, and W is the stored electromagnetic energy per unit length [15]. In the conventional ferruled coupled-cavity slow-wave circuit, the beam is synchronous with only the first RF space harmonic. With $n = 1$, the components of the beam interaction impedance of (1) are obtained at the RF phase-frequency points of the MAFIA-simulated dispersion curve. The first space harmonic magnitude of the on-axis electric field is determined from a Fourier analysis of the total axial electric field on the axis [14]. The stored electromagnetic energy per unit length W is directly calculated by MAFIA, and the group velocity v_g is determined from the local slope of the dispersion curve.

The impedance is more often given in terms of the total impedance, which is defined [16]:

$$Z = \frac{V^2}{2P_{RF}} \tag{3}$$

where V is the gap voltage. It is related to the on-axis beam interaction impedance by [17]:

$$Z = \left[\frac{\beta_n \frac{g}{2}}{\sin\left(\beta_n \frac{g}{2}\right)}\right]^2 (\beta_n L)^2 I_0^2(\gamma_n a) K_n \tag{4}$$

where g is the gap length, I_0 is the modified Bessel function, a is the beam tunnel radius, and

$$\gamma_n = \sqrt{\beta_n^2 - \frac{\omega^2}{c^2}} \tag{5}$$

with ω the angular frequency and c the speed of light.

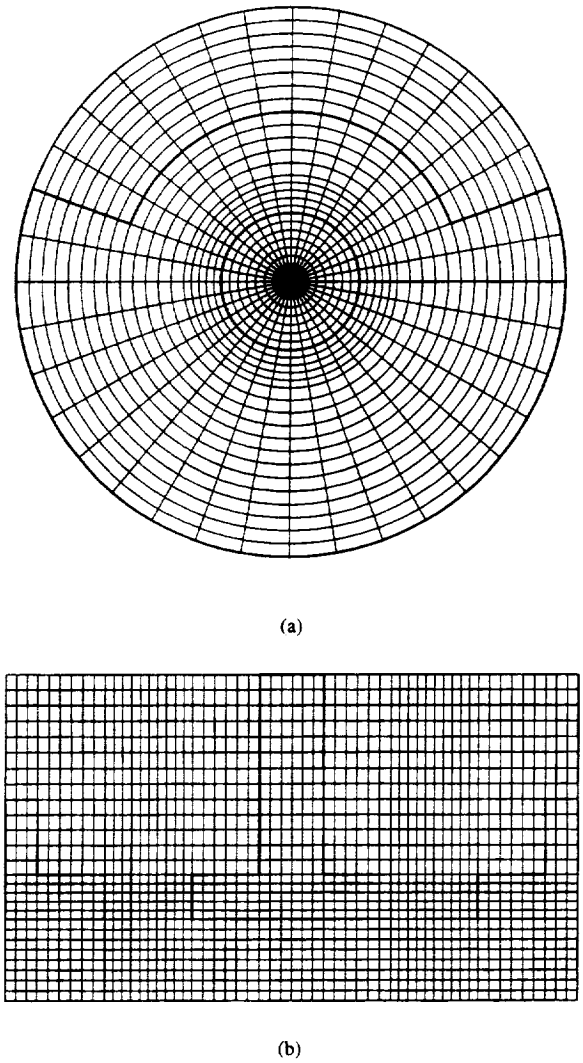

(a)

(b)

Fig. 2. (a) End and (b) cross-sectional MAFIA grid in cylindrical coordinates.

The attenuation in dB/cavity due to the resistive losses of the conducting surfaces can be expressed [18]:

$$\alpha = 8.686 \frac{P_L L}{2W v_g} \tag{6}$$

where L is the cavity length and P_L is the total power loss per unit length which is calculated by MAFIA using a perturbation method with a user-specified value for the surface conductivity. The theoretical value of conductivity for the copper cavity walls at room temperature is $\sigma = 5.8 \times 10^7$ S/m. However, the actual conductivity will be lower than this because of skin, roughness, and work hardening effects [19], [20]. We do not have a measured value of the actual surface conductivity for the 961HA cavities, so in the MAFIA simulations, we assume that it is equal to the value obtained by Tischer [20] at 60 GHz in his measurements on waveguides with highly polished copper surfaces. At 60 GHz, Tischer (Table II and Fig. 9 in [20]) determined that the surface resistivity was a factor of 1.29 higher than the theoretical value. With the conductivity inversely proportional

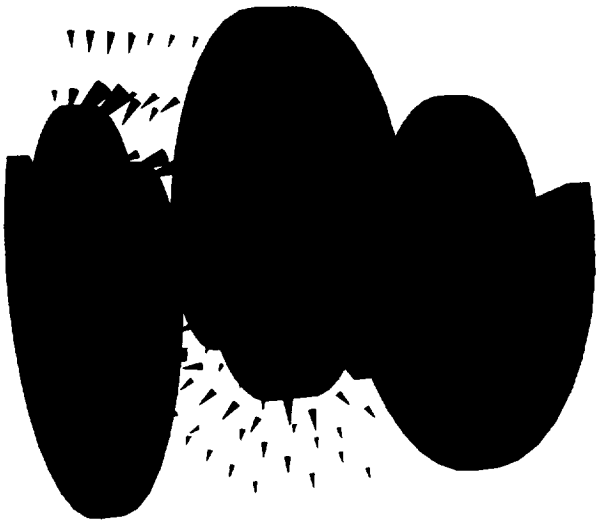

Fig. 3. MAFIA three-dimensional electric field plot for two cavities of Hughes 961HA ferruled coupled-cavity TWT circuit. Size of the three-dimensional arrows is proportional to magnitude of the field. Phase shift per cavity is 225°.

to the square of the surface resistivity, this yields an effective conductivity value of 3.5×10^7 S/m.

B. RF Power

The NASA Coupled-Cavity TWT code, which is based on the one-dimensional formulation of Vaughan [16], is generally designated as 2.5-dimensional in that it models the interaction between a two-dimensional slow-wave RF circuit field and an electron beam with disks or rings of electric charge which have axial, radial, and azimuthal velocity components. The amplitude and phase of the RF circuit field and the trajectories of the electron disks or rings are determined from the calculated axial and radial space-charge, circuit, and magnetic forces as the disks or rings pass through the individual cavities of the circuit. Independent geometrical and electrical parameters are input for each cavity.

Using the values of RF phase shift per cavity, beam interaction impedance and attenuation obtained with MAFIA, the NASA Coupled-Cavity TWT code was used to model the Hughes 961HA TWT circuit. The model consists of a total of 166 RF cavities divided into three sections. The standard cavity has length 0.0968 cm and gap length 0.0292 cm. The input section contains 49 standard cavities, the center section 47 standard cavities, and the output section 46 standard, eleven 2% taper, and seven 4% taper cavities. The sections are separated by severs, with a match cavity on each side. The cavity length and gap are each multiplied by 0.98 and 0.96, respectively, in the 2% and 4% taper cavities. The match cavities are modeled to have dimensions of the standard cavity and the severs are each of length 0.2550 cm.

Simulations were performed at five values of frequency over the V-band range: 59.0, 60.0, 61.5, 63.0, and 64.0 GHz. For each frequency, the MAFIA-derived values of RF phase shift, beam interaction impedance and attenuation were input for the standard, 2% taper, and 4% taper cavities. The match cavities were assigned values of RF phase shift and attenuation equal to that of a standard cavity and impedance equal to one-half the standard value.

The two severs had to be modeled carefully in order to avoid spurious results, especially when simulating at power levels below saturation. To increase the axial grid resolution, each sever was modeled with three cavities. Each of these sever cavities was assigned a loss of 4 dB to give a total of 12 dB loss for each sever. The sever cavities were assigned very small values of beam interaction impedance (0.01 Ohms), and values of phase shift that maintained the RF phase velocity equal to th[illegible]in a standard cavity.

The 73.[illegible] mA, 19.3 kV beam is focused with periodic permanent magnets with a half-period of 0.4880 cm and peak on-axis amplitudes of 0.3500 Tesla (0.1550 Tesla for the first half period). The initial beam/tunnel radius aspect ratio is 0.35. In the simulations, the beam was modeled with 24 disks per RF wavelength. In order to account for the backward wave, the code makes alternating forward and backward integrating passes through the series of cavities [4]. Five round-trip passes were used to obtain convergence. Simulations were repeated with the RF input power successively increased by one dBm increments to obtain the saturation RF output value. For a single simulation at high resolution, the computational time on an IBM RISC/6000 Model 590 Workstation was 285 seconds.

III. Results and Discussion

A. Cold-Test Parameters

Fig. 4 shows the frequency-phase dispersion curves for the cavity mode of the standard cavity simulated in Cartesian and cylindrical coordinates compared to experimental data provided by Hughes Aircraft Company [21]. In both coordinate systems, the calculated RF phase shifts per cavity are higher than experimental values with an absolute average difference across the V-band frequency range of 1.2% in Cartesian coordinates and only 0.3% in cylindrical coordinates. The very significant difference in accuracy can be attributed to the coinciding of the mesh lines in cylindrical coordinates with the boundaries of the barrel and the coupling slots.

Fig. 5 shows the total interaction impedance as a function of frequency. In both coordinate systems, the simulated impedance values are lower than experimental values with an absolute average difference across the V-band frequency range of 8.8% in Cartesian coordinates and only 2.4% in cylindrical coordinates. The improved accuracy in cylindrical coordinates follows from the improved frequency-phase dispersion and subsequently more accurate group velocity calculations.

The attenuation per cavity simulated with an effective surface conductivity value of 3.5×10^7 S/m is shown in Fig. 6. There were no experimental data to compare to the simulated values, but the values calculated in each coordinate system differ from each other by an average of only 1.5%.

B. RF Power Characteristics

The simulated RF power transfer characteristics of the Hughes 961HA TWT at the mid-band frequency of 61.5 GHz

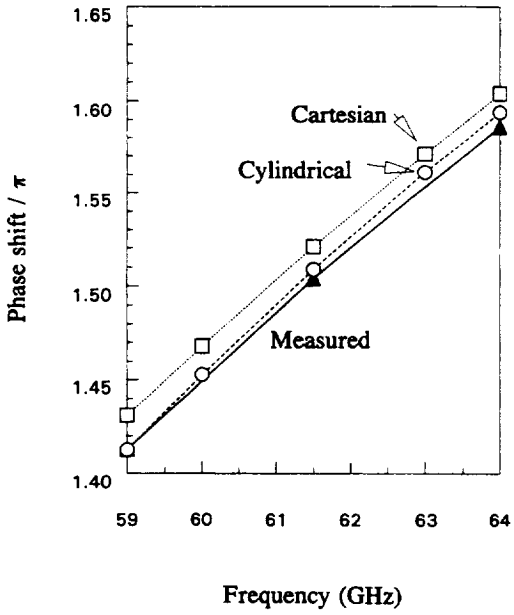

Fig. 4. Frequency-phase dispersion for standard cavity of 961HA circuit. MAFIA simulations in both Cartesian and cylindrical coordinates are compared to measured values.

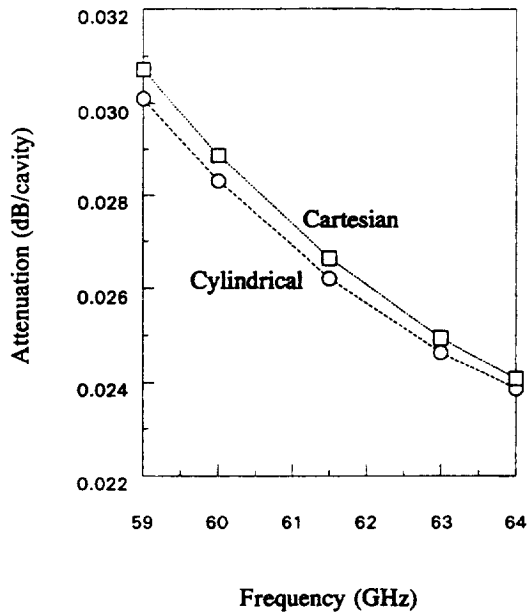

Fig. 6. Simulated attenuation for standard cavity with an effective surface conductivity value of $\sigma = 3.5 * 10^7$. Experimental data was not available.

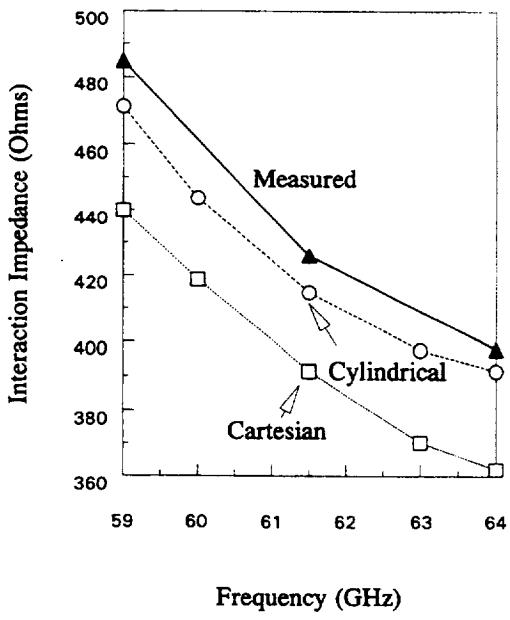

Fig. 5. Total interaction impedance for standard cavity.

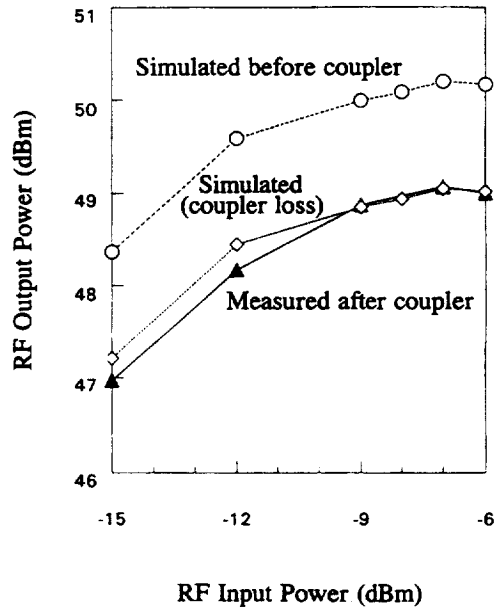

Fig. 7. RF power transfer curve at 61.5 GHz for 961HA circuit. Measured values are shown as measured at the end of a lossy monel coupler waveguide. Results simulated with the NASA Coupled-Cavity TWT Code are shown before the window and coupler at the RF circuit output and with measured window and coupler losses included.

is compared to the measured data [12] in Fig. 7. The top curve shows the simulated power at the end of the RF circuit; however the RF power passes additionally through an alumina output window and a lossy monel (a nickel-copper alloy) output coupler waveguide before measurement. The measured RF power losses at 61.5 GHz are 0.07 dB for the window and 1.08 dB for the coupler [12]. When these power losses are subtracted from the simulated results, the agreement with experimental measurement is excellent. In the simulation, the input power that gives saturation is −7 dBm, the same as the experimental measurement. The saturated output power in watts is 80.7 for the simulation which agrees very well with the experimental value of 80.3.

Fig. 8 shows the RF input power at saturation across the V-band frequency range. The agreement between simulation and experiment is fairly good except at the lower frequency

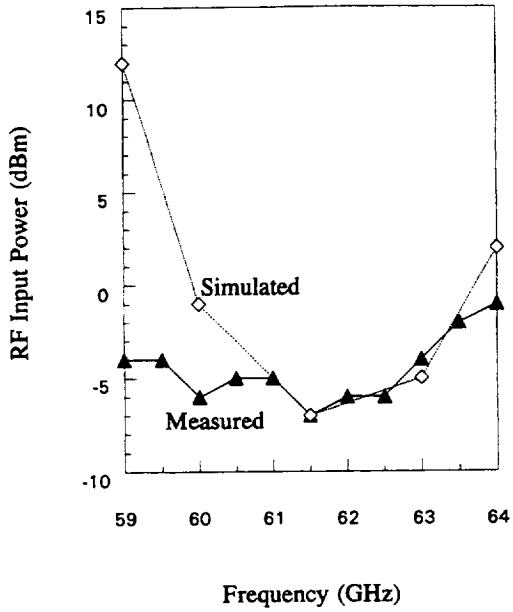

Fig. 8. RF input power at saturation.

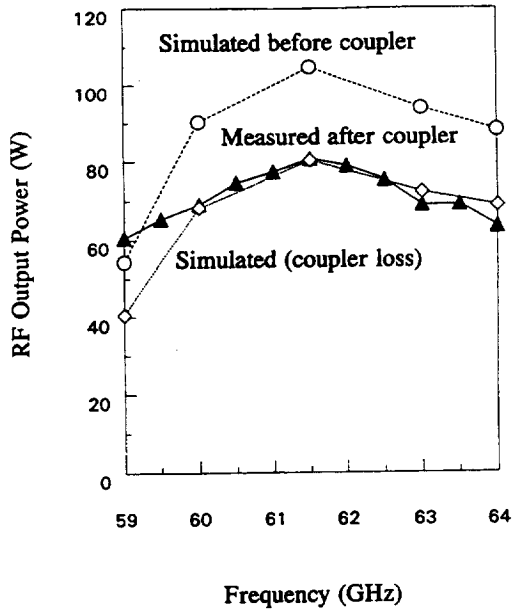

Fig. 9. Saturated RF output power.

band edge. The input power at saturation depends on the overall gain, which is difficult to simulate accurately because a small difference in a cold-test parameter and gain per cavity can accumulate to a fairly large change in overall gain when compounded over a large number of cavities. The simulation is particularly sensitive to small changes in cold-test parameters at the lower frequency band edge.

The corresponding saturated RF output power is shown in Fig. 9. As in Fig. 7, measured RF power losses from the window and coupler are subtracted from the simulated power. With these losses taken into account, the simulated power gives excellent agreement with the experimental data except at the lower frequency band edge. From 60–64 GHz, the average absolute percentage difference between simulated and measured power is only 3.8%.

IV. Conclusions

Procedures have been developed which enable the accurate simulation of the RF output power characteristics for coupled-cavity TWT's. A beam-RF interaction code is used with cold-test parameters obtained from the three-dimensional electromagnetic simulation code MAFIA. These cold-test parameters (RF phase shift per cavity, impedance, and attenuation) and the subsequent RF output power characteristics were computed and compared to experimental data for an existing V-band (59–64 GHz), 75-Watt coupled-cavity TWT, the Hughes Aircraft Company Model 961HA.

The MAFIA simulations were performed in both Cartesian and cylindrical coordinates and compared to measured results for RF phase shift per cavity and impedance across the V-band frequency range. The agreement with experiment was substantially better with cylindrical coordinates; the absolute average differences for phase shift were 0.3% compared to 1.2% with Cartesian coordinates and for impedance were 2.4% compared to 8.8%. There were no experimental data to compare with the attenuation computations. In these simulations, an effective surface resistivity was used to take into account skin, roughness, and work hardening effects of the copper surfaces.

With the cold-test parameters calculated in MAFIA with cylindrical coordinates as input, the NASA Coupled-Cavity TWT Code was used to simulate the 166-cavity RF circuit of the 961HA across the V-band frequency range. Taking into account the output window and coupler loss, the agreement with experiment was very good except at the lower frequency band edge. From 60–64 GHz, the average absolute percentage difference between simulation and experiment was only 3.8%.

This paper shows that the saturated RF output power of a coupled-cavity TWT can be accurately simulated without the need of experimentally obtaining cold-test parameters. The procedures demonstrated in this paper enable the design of coupled-cavity TWT slow-wave circuits with significantly less dependence on expensive and time-consuming experimental cold-testing procedures. Previously the expense and time involved in developing a new circuit resulted in very conservative designs involving relatively incremental modifications to existing successful circuits. Now novel circuit designs such as [22] can be much more readily investigated. This new capability should result in substantially higher performances at lower development costs.

References

[1] D. J. Connolly and T. A. O'Malley, "Computer program for analysis of coupled-cavity traveling-wave tubes," NASA, TN D-8492, 1977.
[2] T. A. O'Malley and D. J. Connolly, "Users' manual for computer program for one-dimensional analysis of coupled-cavity traveling-wave tubes," NASA, TM X-3565, 1977.
[3] T. A. O'Malley, "Users' manual for computer program for three-dimensional analysis of coupled-cavity traveling-wave tubes," NASA, CR-168269, 1984.

[4] J. D. Wilson, "Revised NASA axially symmetric ring model for coupled-cavity traveling-wave tubes," NASA, TP 2675, 1987.
[5] ——, "Computationally generated velocity taper for efficiency enhancement in a coupled-cavity traveling-wave tube," *IEEE Trans. Electron Devices*, vol. 36, pp. 811–816, Apr. 1989.
[6] K. Amboss, J. Davis, K. Hively, R. Ripley, C. Thorington, and J. Wilson, "A 50 kW peak-power 4 kW average power moderate confined-flow, PPM-focused X-band TWT," in *IEEE Int. Electron Devices Meet.*, Washington, DC, Dec. 3–6, 1989.
[7] J. D. Wilson, H. C. Limburg, J. A. Davis, I. Tammaru, and J. P. Vaszari, "A high efficiency ferruleless coupled-cavity traveling-wave tube with phase-adjusted taper," *IEEE Trans. Electron Devices*, vol. 37, pp. 2638–2643, Dec. 1990.
[8] J. D. Wilson, P. Ramins, and D. A. Force, "Spent beam refocusing analysis and multistage depressed collector design for a 75-W, 59- to 64-GHz coupled-cavity traveling-wave tube," NASA, TP 3039, 1990.
[9] T. Weiland, "On the numerical solution of Maxwell's equations and applications in the field of accelerator physics," *Part. Accel.*, vol. 15, pp. 245–292, 1984.
[10] ——, "On the unique numerical solution of Maxwellian eigenvalue problems in three dimensions," *Part. Accel.*, vol. 17, pp. 227–242, 1985.
[11] C. L. Kory and J. D. Wilson, "Three-dimensional simulation of traveling-wave tube cold-test characteristics using MAFIA," NASA, TP 3513, 1995.
[12] H. C. Limburg, D. E. Zamora, J. A. Davis, and I. Tammaru, "75 Watt, 59- to 64-GHz space TWT," draft of NASA Contractor Report NAS3-25090, 1995.
[13] F. Kantrowitz and I. Tammaru, "Three-dimensional simulation of frequency-phase measurements of arbitrary coupled-cavity RF circuits," *IEEE Trans. Electron Devices*, vol. 35, pp. 2018–2026, Nov. 1988.
[14] J. W. Maruschek, C. L. Kory, and J. D. Wilson, "Generalized three-dimensional simulation of ferruled coupled-cavity traveling-wave tube dispersion and impedance characteristics," NASA, TP 3389, 1993.
[15] J. W. Gewartowski and H. A. Watson, *Principles of Electron Tubes*. Princeton, NJ: Van Nostrand, 1965, p. 357.
[16] J. R. M. Vaughan, "Calculation of coupled-cavity TWT performance," *IEEE Trans. Electron Devices*, vol. ED-22, pp. 880–890, Oct. 1975.
[17] D. J. Connolly, "Determination of the interaction impedance of coupled cavity slow wave structures," *IEEE Trans. Electron Devices*, vol. ED-23, pp. 491–493, May 1976.
[18] O. P. Gandhi, *Microwave Engineering and Applications*. New York, NY: Pergamon, 1981, p. 24.
[19] F. J. Tischer, "Excess conduction losses at millimeter wavelengths," *IEEE Trans. Microwave Theory and Techniques*, vol. MTT-24, pp. 853–858, Nov. 1976.
[20] ——, "Experimental attenuation of rectangular waveguides at millimeter wavelengths," *IEEE Trans. Microwave Theory and Techniques*, vol. MTT-27, pp. 31–37, May 1976.
[21] A. L. Rousseau, Hughes Aircraft Company, personal communication, 1988.
[22] C. L. Kory and J. D. Wilson, "Novel high-gain, improved-bandwidth, finned-ladder V-band traveling-wave tube slow-wave circuit design," *IEEE Trans. Electron Devices*, vol. 42, pp. 1686–1692, Sept. 1995.

Jeffrey D. Wilson (M'87), for a photograph and biography, see p. 1692 of the September 1995 issue of this TRANSACTIONS.

Carol L. Kory (M'95), for a photograph and biography, see p. 1692 of the September 1995 issue of this TRANSACTIONS.